Polarization-dependent oxygen, vacancy distribution in ferroelectric Hf0.5 Zr0.5 O2 capacitors

Gunjan Yadav, Lucía Pérez Ramírez, Nick Barrett, Jean Coignus, Nicolas Vaxelaire, Laurent Grenouillet, Jean Pascal Rueff, Denis Ceolin

Polarization-dependent, oxygen vacancy distribution in ferroelectric $Hf_{0.5}Zr_{0.5}O_2$ capacitors

Gunjan Yadav[1], Lucía Pérez Ramírez[1] and Nick Barrett[1]
[1]SPEC, CEA, CNRS, Université Paris-Saclay,
F-91190 Gif-sur-Yvette, France
nick.barrett@cea.fr

Jean Coignus[2], Nicolas Vaxelaire[2] and Laurent Grenouillet[2]
[2]CEA, Leti, Univ. Grenoble-Alpes
Grenoble, France

Jean Pascal Rueff[3] and Denis Ceolin[3]
[3]Synchrotron SOLEIL, L'Orme des Merisiers,
Départementale 128,
91190 Saint-Aubin, France

2024 22nd Non-Volatile Memory Technology Symposium (NVMTS) | 979-8-3315-3265-9/24/$31.00 ©2024 IEEE | DOI: 10.1109/IEEECONF63530.2024.10830905

***Abstract*— The discovery of ferroelectricity in hafnia-based thin films has paved the way for their integration into non-volatile memory technologies, offering compatibility with CMOS processes and the potential for aggressive scaling. One significant aspect impacting the reliability and performance of ferroelectric $Hf_{0.5}Zr_{0.5}O_2$ (HZO) capacitors is the oxygen vacancy (V_O) concentration, which influences endurance, retention, and polarization stability. This study investigates the V_O concentration profile for the woken-up state (10^4 cycles) in HZO-based ferroelectric capacitors (FeCAPs) in different polarization states ($P^{\uparrow}$ and $P^{\downarrow}$). The V_O distribution is quantified using Hard X-ray photoemission spectroscopy (HAXPES), using incident photon energies from 3 to 9 keV to calculate the V_O concentration profile across the HZO layer non-destructively. Results indicate that V_O accumulates near the top TiN/HZO interface for the $P^{\downarrow}$ state, while they drift toward the bottom HZO/TiN interface for the $P^{\uparrow}$ state under the effect of the internal polarization field. This polarization-dependent V_O distribution correlates with voltage and field offsets observed in electrical measurements, providing insights into defect mobility that can inform FeRAM device optimization. Our results show that the polarization behavior, i.e. the alignment and stability of electric dipoles within the HZO layer, strongly correlates with the distribution of V_O, which plays a crucial role in enhancing the reliability and performance of ferroelectric memory devices. These findings enhance our understanding of the coupling between defect chemistry and ferroelectric properties in HZO, supporting the engineering of high-performance, CMOS-compatible ferroelectric memory technologies.**

Keywords-HZO, HAXPES, FeRAM, Polarization, Oxygen vacancies

I. INTRODUCTION

The discovery of ferroelectricity in doped hafnium oxide (HfO_2) thin films has revolutionized the field of emerging, non-volatile memory technologies, offering a path toward energy-efficient, high-density ferroelectric random-access memories (FeRAMs) compatible with CMOS processes. Since the seminal work by Böscke et al. (2011), which demonstrated ferroelectricity in hafnia for the first time, the focus has shifted toward optimizing device performance parameters such as endurance, retention, and switching characteristics to meet the demands of next-generation memory applications [1]. Fatigue, wake-up, and imprint effects are fundamental concerns in ferroelectric research, as they impact the long-term reliability and performance of memory and logic devices. Fatigue results in polarization degradation with repeated cycling, wake-up phenomena enhance polarization stability initially, and imprint causes shifts in polarization behavior over time, affecting data retention and polarization stability. Understanding these effects is essential for developing robust and high-endurance ferroelectric technologies. Among the challenges, the behavior of oxygen vacancy (V_O) concentration in these materials has emerged as a critical factor influencing the stability and reliability of ferroelectric states, thus necessitating a deeper investigation into the distribution and dynamics of V_O under different polarization conditions (cycling, imprints etc.)[2].

Several groups have explored the role of V_O in HZO-based ferroelectric devices, providing insight into how these defects influence ferroelectric properties. For instance, Materano et al. (2020) studied the impact of V_O on ferroelectric switching and endurance, highlighting that a controlled distribution of vacancies can significantly enhance device reliability [3]. This study, along with others by Grenouillet et al. (2020) and Barrett et al. (2024) explains the complex interplay between V_O distribution and polarization stability, proposing that selective engineering of V_O profiles could mitigate common issues such as polarization fatigue and imprint [4][5].

X-ray photoelectron spectroscopy (XPS) is a powerful tool for the analysis of the chemical and electronic structure of HZO, allowing for non-destructive depth profiling of V_O. The fraction of reduced Hf is a quantitative signature of the V_O concentration since each V_O releases two electrons which then reduce neighboring cations giving a distinct core level component. For example, the core level binding energy of the Hf^{3+} component is shifted by ~ 1 eV to lower energy with respect to that of Hf^{4+} [2]. However, XPS is also extremely surface sensitive, typically

probing up to ~3-5 nm making it difficult to study ferroelectric layers below a realistic top electrode. By exciting the same core level with hard X-rays (HAXPES), the probing depth can be increased by an order of magnitude to ~20-30 nm [6].For example, Zhou et al. utilized HAXPES to identify V_O migration in ferroelectric HZO capacitors under an applied electric field [7]. Barrett et al. have quantified the Vo profile due to oxygen scavenging in Si-doped HfO_2-based FeCAPs [5]. This method offers an advantage over depth profiling by traditional XPS, which requires sputtering that can induce surface artefacts and complicate the interpretation of vacancy concentration profiles. By employing HAXPES at variable photon energies, one can obtain non-invasive, depth-resolved data, leading to an accurate representation of the V_O gradient within the HZO layer [8].

In our current study, we focus on quantifying V_O distribution in HZO capacitors as a function of polarization state ($P^{\uparrow}$ and $P^{\downarrow}$) of the FeCAP after wake-up cycling. The woken up state is reached when the domain structure has been fully unpinned and the associated V_O are free to migrate. Building on the methodologies established in prior work, our approach uses HAXPES with a tunable photon energy range (3 to 9 keV) to measure the V_O concentration profile from Hf 3d core level spectra. Our findings demonstrate a direct correlation between V_O accumulation near the electrode interfaces and the polarization state, which could impact long-term retention and field stability in FeRAM devices. Notably, we observe that for the $P^{\downarrow}$ polarization state, V_O tend to accumulate near the top electrode interface, while for the $P^{\uparrow}$ state, these vacancies migrate toward the bottom interface. This migration behavior aligns with the studies conducted by Takahashi et al. (2021), who suggested that the distribution of V_O can be engineered through interface modifications which influence the internal electric field to optimize polarization stability [9].

In addition, our results provide an understanding of the V_O movement under internal fields in HZO and a methodology framework for further studies aimed at enhancing device performance via materials engineering. This work aligns with recent efforts in the field, who have emphasized the need for reliable, non-destructive methods for vacancy profiling to improve the reliability and scalability of ferroelectric memories [10][11]. In summary, we present an analysis of the polarization-dependent V_O distribution in fully woken up HZO capacitors, utilizing HAXPES to provide an unique insight into the role of V_O in ferroelectric performance. The results will support the design of robust, scalable, and energy-efficient non-volatile memory devices, underlining the potential for HZO-based FeRAM as a promising solution for next-generation, low-power memory applications.

II. Methodology

The fabrication of HZO FeCAPs was carried out using atomic layer deposition (ALD) at 300°C to achieve a 10 nm-thick HZO layer, sandwiched between two 10 nm TiN electrodes deposited via chemical vapor deposition (CVD) at CEA/LETI (Grenoble). Post-deposition, the devices were subjected to rapid thermal

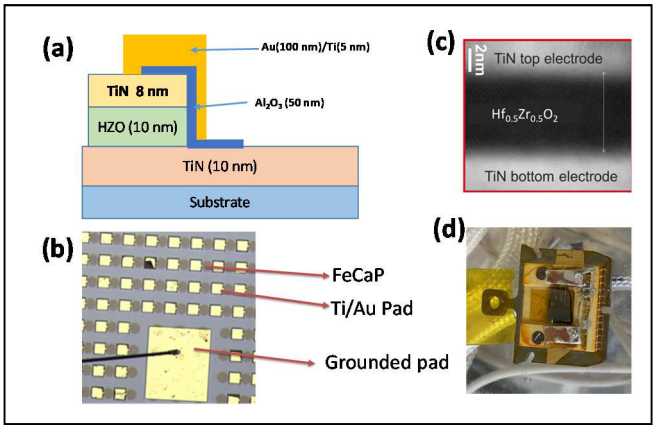

Figure 1. (a) Schematic cross-section of the HZO capacitor structure with TiN top and bottom electrodes and the HZO ferroelectric layer. (b) Top view of a field of capacitor structures with Ti/Au connecting pads and (c) cross sectional TEM image of the sample (d) Image of the SHOMEC13 sample holder.

annealing (RTA) at 450°C for 1 minute in an inert N_2 atmosphere to promote crystallization of the HZO layer in the ferroelectric orthorhombic phase. A short fabrication loop has been set-up to fabricate patterned HZO-based FeCAPs of diameter 100 x 100 μm^2 and electrically characterize them. The capacitor fields was further processed at the C2N laboratory (Palaiseau, France) using Ion Beam Etching (IBE) to remove the HZO layer between capacitors.

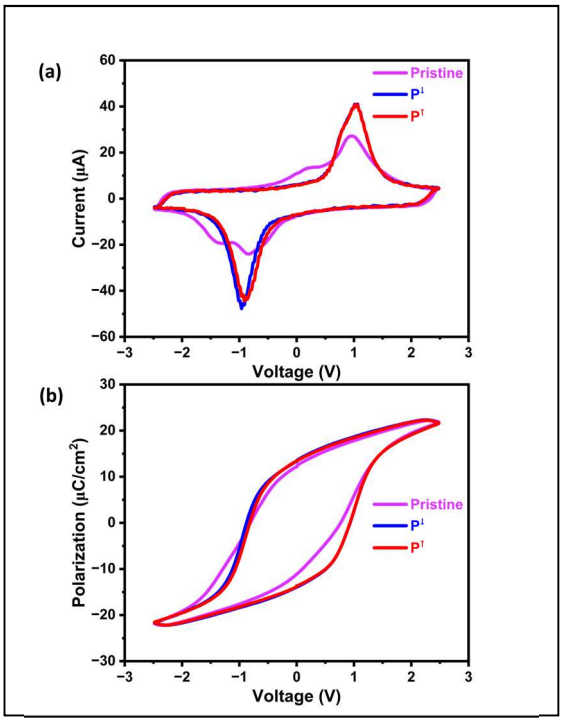

Figure 2. (a) P-E and (b) I-V characteristics curve from pristine and fully woken up state.

Following this, at CEA/SPEC, maskless lithography (μMLA 100) was used to deposit an Al_2O_3 insulating layer onto the patterned FeCAP sample. Subsequently, metal contact pads made of Ti/Au were deposited on top of the Al_2O_3 layer providing an ohmic contact with the top electrode (Figure 1 (a) and 1 (b)). This geometry allows reliable cycling of individual capacitors whilst leaving the TiN top electrode intact and the underlying capacitor available for the HAXPES analysis.

Following fabrication, an initial electrical "wake-up" process was conducted to stabilize the ferroelectric domains, cycling the capacitors 10^4 times at 2.5V to eliminate domain pinning and imprint effects and ensure stable, repeatable switching characteristics and high V_O mobility. The devices were then polarized into well-defined upward ($P^{\uparrow}$) or downward ($P^{\downarrow}$) polarization states. Finally, the top and bottom electrodes were wire-bonded to the pins of the SHOMEC13 (Ferrovac) holder (Fig. 1(d)). During HAPES experiments top and bottom electrodes can thus be grounded avoiding any sample charging under the synchrotron beam.

Electrical characterizations, including polarization-electric field (P-E) hysteresis and current-voltage (I-V) measurements, were conducted to verify the ferroelectric properties and assess leakage behavior using the aixACCT TF1000 Ferro tester at CEA/SPEC.

Structural characterizations were performed using two complementary X-ray diffraction techniques at CEA/LETI. In-plane X-ray diffraction (IPXRD) measurements were carried out on a Rigaku SmartLab® system, while grazing incidence XRD (GIXRD) experiments were conducted using a PANalytical Empyrean® diffractometer. In both case, diffraction patterns were collected over a 2θ range of 20° to 38° using a parallel incident X-ray beam, collimated by a mirror, and Cu Kα radiation (λ = 1.5406 Å).

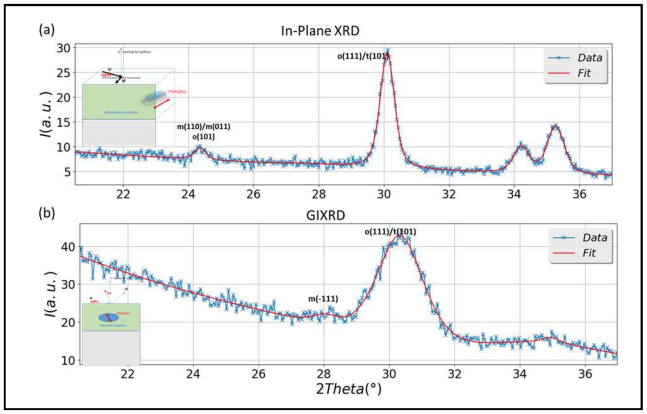

Figure 3. XRD spectra of TiN/HZO/TiN/Si sample in (a) in-plane and (b) GIXRD configuration.

Table1. Parameters calculated from the XRD spectra for TiN/HZO/TiN/Si.

scattering vector	2θ (°)	d (Å)	fwhm (°)	l(nm)
GIXRD	30.31	2.946	1.71	5.0
in-plane	30.08	2.969	0.51	17.2

Hf 3d HAXPES core level spectra were recorded at the GALAXIES beamline of the SOLEIL synchrotron for quantification of the V_O concentration as a function of both depth and polarization state. By varying the photon energy from 3 to 9 keV, we achieved characteristic probing depths ranging from approximately 3.1 nm to 7.6 nm into the HZO layer, as calculated by as calculated by the (TPP-2M) algorithm allowing for a detailed V_O profile across the 10 nm HZO layer thickness [12]. The characteristic probing depth is defined as the depth from which half of the total Hf 3d signal comes from. The binding energy calibration is performed setting the Au $4f_{7/2}$ peak binding energy due to photoemission from the Au/Ti pad in ohmic contact with the top electrode at 84.0 eV.

III. Results and Discussion

A. Electrical Characterization

Fig. 2 shows the I-V (a) and P-E (b) characteristics of the HZO capacitors. I-V characteristics show sharp current switching peaks (after wake-up) at voltages corresponding to the coercive fields and two separate current peaks in a pristine state. The double peak structure is commonly associated with antiferroelectric (AFE) ordering. In these systems, the polarization domains are pinned in specific configurations, leading to a characteristic double peak in I-V curve[13]. After repeated electrical cycling (the wake-up process), the defects and oxygen vacancies redistribute more uniformly, and the internal field stabilizes. This results in improved domain alignment means the electric dipoles are oriented in a preferred direction and polarization switching, manifesting as a single, more intense current peak, characteristic of the ferroelectric state. The current (-42 and -43 μA) and position (-0.81 and -0.93 V) variations of these peaks between the $P^{\uparrow}$ and $P^{\downarrow}$ polarization states indicate an asymmetric switching process [14]. The observed switching asymmetry is attributed to a built-in electric field resulting from the non-uniform distribution of defects and/or variations at the electrode interfaces [15]. The internal field shifts the coercive voltages and modulates the energy barriers for polarization reversal, thereby affecting the intensity and position of the switching current peaks. Moreover, the asymmetric distribution of V_O further influences the polarization switching dynamics by altering the nucleation rates and propagation mechanism of ferroelectric domains, leading to non-uniform switching behavior [9][16].

The P-E loop shows a classic ferroelectric response, where the polarization switches direction as the applied voltage exceeds the coercive voltages at around ±1.5 V. The polarization observed is approximately ±20 μC/cm². The asymmetry in coercive fields between the $P^{\uparrow}$ and $P^{\downarrow}$ polarization states confirms the 0.06 V imprint observed in the I-V characteristic of Fig.2(a). Given that both electrodes are TiN, an uneven distribution of charged V_O, could be responsible for imprinting the polarization switching behavior.

B. Structural Analysis

The in-plane XRD diffractogram (Fig. 3a) reveals the structural arrangement of the film along in-plane direction. The sharp and well-resolved peaks indicate high crystallinity, with minimal defects and well-ordered domains along this direction. In this geometry, the shallow angle of the X-ray beam relative to

the surface interacts with a larger in-plane volume of the film, effectively increasing the diffracting volume for thin films, such as the 10 nm sample studied. This enhances the intensity of the in-plane diffraction peaks.

In contrast, the GIXRD diffractogram (Fig. 3b) represents the scattering plane closer to the out-of-plane direction (e.g., tilted by 15° for the o/t peak), providing insights into the vertical alignment and ordering of the crystal lattice. The GIXRD pseudo-out-of-plane configuration exhibits a broader full-width at half maximum (FWHM) of 1.71° and a smaller coherence length of 5.0 nm, indicative of reduced crystalline order and greater structural imperfections or variations in lattice spacing, possibly due to strain or defects along this direction. Conversely, the in-plane measurement shows a much narrower FWHM of 0.51° and a larger coherence length of 17.2 nm, signifying a more uniform and well-ordered crystal lattice along this orientation (Table 1).

C. Hf 3d core level analysis of VO distribution

HAXPES provided a quantitative, depth profile analysis of the V_O distribution across the HZO layer. By setting the photon energies at 3, 5, 7 and 9 keV, HAXPES allowed non-destructive characterization from the top TiN/HZO interface region to the bottom HZO/TiN interface. The characteristic probing depth (z_c) is calculated from the expression for the Hf core-level attenuated intensity deduced from the Beer-Lambert law, $I_{\mathrm{Hf}} = \int_0^{\infty} e^{-d/\lambda} \mathrm{d}z$, where λ is the inelastic mean free path of the electrons calculated by the (TPP-2M) algorithm[12]. z_c is defined as the depth at which this intensity is attenuated by half [17] and is equal to λ ln2. Figure 4 shows the Hf 3d core-level spectra at the four different photon energies, for capacitors in and $P^{\downarrow}$ (left panels) and $P^{\uparrow}$ (right panels) states after cycling. The spectra were fitted using Gaussian-Lorentzian (GL(70))peak shapes, with a main component at 1662 eV, which corresponds to the Hf^{4+} from the stoichiometric oxide, and two components at lower binding energy with core-level shifts of –1.6 eV and -3.2 eV, which correspond to reduced hafnium atoms in the Hf^{3+} and $^{2+}$ state, respectively.

Each Vo provides two free electrons, thus reducing two Hf^{4+} atoms to two Hf^{3+} or one Hf^{2+}. Hence, given the $Hf_{0.5}Zr_{0.5}O_2$ stoichiometry (Hf:O=1:4), the Vo concentration can be calculated from the Hf 3d core level intensities of Hf^{4+}, Hf^{3+} and Hf^{2+} as follows,

$$Vo = \frac{I(\mathrm{Hf}^{3+})}{I(\mathrm{Hf_{total}})} \times \frac{1}{8} + \frac{I(\mathrm{Hf}^{2+})}{I(\mathrm{Hf_{total}})} \times \frac{1}{4}.$$

The factors 1/8 and 1/4 coefficients are due to the stoichiometric ratio of Hf to O.

The results are plotted in Fig. 5 as a function of the characteristic probing depth as determined by the incident photon energy. A notable increase in V_O concentration was observed near the top TiN/HZO interface for the $P^{\downarrow}$ state, while for the $P^{\uparrow}$ state, V_O migrated toward the bottom HZO/TiN interface. This behavior indicates a polarization-dependent redistribution mechanism, where V_O tend to accumulate at the interface opposite to the polarization vector. Such migration suggests that an internal electric field drives the positively charged V_O movement. As the FeCAPs are grounded the electric field driving the V_O migration must be internal to the HZO [6][7]. The accumulation of V_O at one interface or the other creates an additional internal field in the same direction as the existing polarization state, i.e. opposite to any depolarizing field.

D. Influence of V_O *Distribution on Device Performance*

The relationship between V_O distribution and electrical performance is critical to understanding ferroelectric stability and imprints. The increased V_O concentration near the top interface in the $P^{\downarrow}$ state likely stabilizes the downward polarization by enhancing the local electric field near the interface, reducing the energy barrier for switching. The V_O migration toward the bottom interface in the $P^{\uparrow}$ state reinforces the upward polarization, reducing the potential for depolarization effects over time. This symmetric distribution-dependent stability is essential for FeRAM endurance and retention, as it supports the formation of robust polarization states. These results suggest that controlled manipulation of oxygen vacancy concentrations through interface engineering could enhance device performance by stabilizing polarization states, which is crucial for memory applications. The Vo concentrations at the top and bottom interfaces are not identical—for instance, in this case, they are 1.16% and 1.24%, respectively. The difference in Vo distribution contributes to a built-in electric field that reinforces and stabilizes the polarization states, thereby supporting reliable polarization switching. On the other hand, it also creates an imprint in the P-E loop which if too big may become detrimental to device operation. The electric field created by the difference in oxygen vacancy concentration (ΔVo=0.16% and 0.2% for $P^{\uparrow}$ and $P^{\downarrow}$) is calculated using Poisson's equation [18]:

$$\frac{d\varphi^2}{dx^2} = -\frac{\rho}{\epsilon}; E = -\frac{d\varphi}{dx};\ \rho = q \times n; n = \Delta V_o \times N_{sites}; \epsilon = \epsilon_o . \epsilon_r; E = \frac{q \times \Delta V_o \times N_{sites} \times x}{\epsilon_o \times \epsilon_r} = 211 \times \Delta V_o \left(\frac{MV}{cm}\right).$$

Here, ϕ(x) is Electric potential as a function of position, ρ is the charge density, ϵ is the permittivity, ϵ_o is the permittivity in free space ($8.85\text{x}10^{-12}$ F/m), ϵ_r is the relative permittivity of HZO (~25)[19], n is the concentration of oxygen vacancies in cm^{-3}, N_{sites} is the number of potential oxygen sites per unit volume in HZO, $\frac{8}{137} \times 10^{30} m^{-3}$ [20], x= $5\times 10^{-10} m$ (Assuming that the oxygen vacancies are distributed along the first unit cell at the interface), ΔVo is the oxygen vacancy concentration difference, q is the elementary charge (1.6×10^{-19} C).

The electric field created is approximately 0.34 and 0.42 MV/cm for $P^{\uparrow}$ and $P^{\downarrow}$ at the top interface.

E. Advantages of Non-Destructive HAXPES Profiling

Using HAXPES for non-destructive depth profiling provided distinct advantages over conventional sputtering techniques used for depth profiling which often introduce artefacts that complicate interpretation. In particular, Ar ion sputtering preferentially removes oxygen, thereby reducing the remaining cations. An observed increase in V_O concentration deduced from the intensity of the reduced Hf core level component may well be produced by the sputtering process and have nothing to do with the true V_O concentration [21].

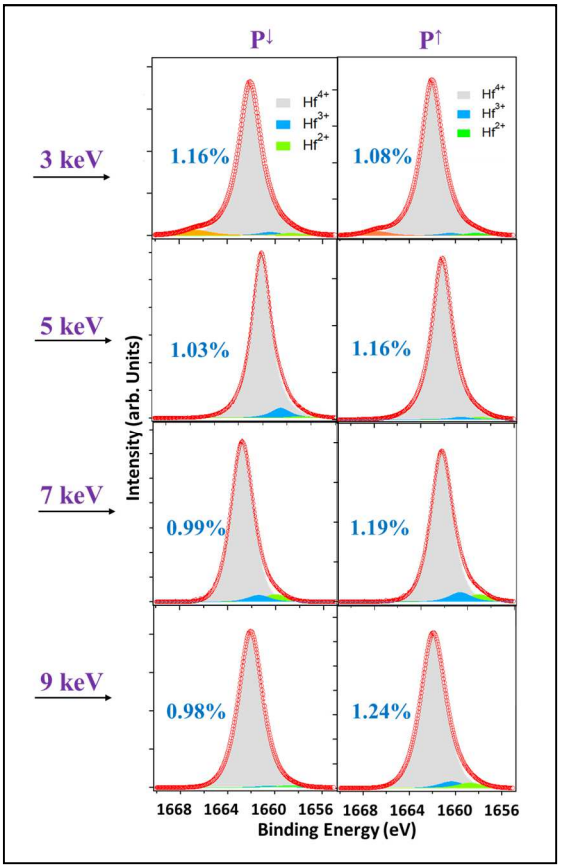

Figure 4. HAXPES spectra for the Hf 3d core level at photon energies of 3 keV and 9 keV, showing the V_O concentration profile differences between the $P^{\uparrow}$ and $P^{\downarrow}$ polarization states.

By varying the photon energy, HAXPES facilitated a precise, artefact-free characterization of V_O concentration across the HZO layer, offering insights into the internal defect dynamics without compromising structural integrity. This methodological approach positions HAXPES as a powerful tool for studying oxygen vacancies in ferroelectric thin films, providing reliable, in-depth characterization essential for advancing memory device technology [9].

F. Implications for Device Optimization

The findings presented here highlight the critical impact of V_O concentration and kinetics under the internal polarization field on the ferroelectric properties of HZO capacitors. The Polarization-dependent V_O distribution observed across the HZO layer provides a foundation for future work on V_O control through advanced material and interface engineering. By tailoring V_O profiles to enhance polarization stability and minimize switching degradation, this approach offers a pathway to improved FeRAM performance and scalability. Future studies may further explore V_O management techniques, including bias conditioning and layer stacking, in particular oxide interface layers to inhibit or metallic layers to enhance oxygen scavenging and hence V_O concentration and thus to optimize ferroelectric stability in HZO-based memory devices.

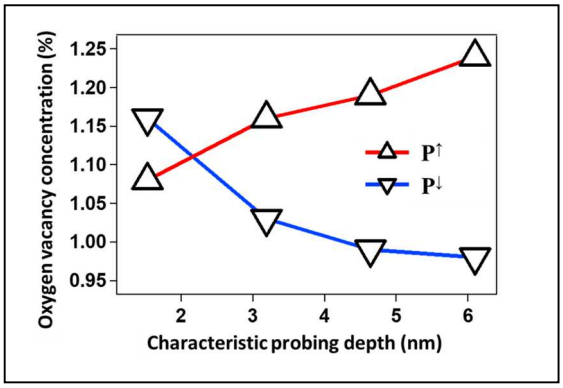

Figure 5. Depth-resolved Vo concentration profile across the HZO layer, with accumulation near the top electrode interface in the $P^{\downarrow}$ state and migration toward the bottom interface in the $P^{\uparrow}$ state

IV. CONCLUSION

This study demonstrates the importance of Vo migration in shaping the polarization behavior of HZO ferroelectric capacitors. The P-E hysteresis loops exhibited robust retention and endurance, with remanent polarization values of 20 μC/cm² for the $P^{\uparrow}$ state and 18 μC/cm² for the $P^{\downarrow}$ state, well suited for memory applications. I-V measurements indicated low leakage currents, emphasizing the dielectric stack's long-term stability. Depth-resolved HAXPES profiling is sensitive to polarization state and changes in V_O distribution due to drift under internal field. It provides an accurate Vo concentration profile across the 10 nm HZO layer, avoiding artefacts typically introduced by Ar^+ sputtering in conventional XPS. The Vo concentration increases with increasing photon energy from 3 to 9 keV in the $P^{\downarrow}$ state and increases with increasing photon energy for the $P^{\uparrow}$ state. These findings suggest that Vo migration within the TiN/HZO/TiN structure is crucial for stabilizing polarization states and enhancing ferroelectric reliability. The insights gained underscore the potential of HZO-based devices for scalable, high-performance electronic applications. HAXPES can be used to quantitatively scan the V_O distribution in a comprehensive library of sample compositions and process parameters providing a reliable methodology for materials engineering of ferroelectric properties.

ACKNOWLEDGEMENT

The authors would like to thank the Agence National de la Recherche for its financial support through the France 2030 project under Grant ANR-22-PEXD-0018 and from the European Union project 101135656 Ferro4EdgeAIThis work was carried out at the GALAXIES beamline of the SOLEIL Synchrotron, and the authors gratefully acknowledge the support and resources provided by the nanofabrication facility at CEA/SPEC and the IBE etching at C2N (Dr. Feriel Laourine).

REFERENCES

[1] T. S. Böscke, J. Müller, D. Bräuhaus, U. Schröder, and U. Böttger, "Ferroelectricity in hafnium oxide thin films," *Appl. Phys. Lett.*, vol. 99, no. 10, 2011.

[2] W. Hamouda *et al.*, "Physical chemistry of the

TiN/Hf0. 5Zr0. 5O2 interface," *J. Appl. Phys.*, vol. 127, no. 6, 2020.

[3] M. Materano *et al.*, "Polarization switching in thin doped HfO2 ferroelectric layers," *Appl. Phys. Lett.*, vol. 117, no. 26, 2020.

[4] L. Grenouillet *et al.*, "Oxygen vacancy distribution in HZO and impact on memory performance," in *Proceedings of the IEEE Symposium on VLSI Technology*, 2020.

[5] N. Barrett *et al.*, "Oxygen vacancy engineering in Si-doped, HfO2 ferroelectric capacitors using Ti oxygen scavenging layers," *Appl. Phys. Lett.*, vol. 125, no. 4, 2024.

[6] C. S. Fadley, "Hard X-ray photoemission: An overview and future perspective," *Hard X-ray Photoelectron Spectrosc.*, pp. 1–34, 2016.

[7] X. Zhou, H. Li, J. Wang, L. Chen, and Y. Wang, "Depth profiling of oxygen vacancies in HZO using HAXPES," *J. Appl. Phys.*, vol. 132, no. 3, p. 33102, 2022.

[8] A. Mallick, M. K. Lenox, T. E. Beechem, J. F. Ihlefeld, and N. Shukla, "Oxygen vacancy contributions to the electrical stress response and endurance of ferroelectric hafnium zirconium oxide thin films," *Appl. Phys. Lett.*, vol. 122, no. 13, 2023.

[9] Y. Takahashi, T. Yamamoto, M. Kinoshita, and K. Nakazato, "Interface engineering for optimized VO distribution in ferroelectric HZO capacitors," *IEEE Trans. Electron Devices*, vol. 68, no. 7, pp. 3085–3092, 2021.

[10] R. Alcala *et al.*, "BEOL Integrated Ferroelectric HfO_2-Based Capacitors for FeRAM: Extrapolation of Reliability Performance to Use Conditions," *IEEE J. Electron Devices Soc.*, vol. 10, pp. 907–912, 2022.

[11] N. Barrett, J.-P. Rueff, L. Grenouillet, and D. Ceolin, "Challenges and advances in ferroelectric memory technology," in *Proceedings of the Ferroelectric Materials Symposium*, 2023.

[12] S. Tanuma, C. J. Powell, and D. R. Penn, "Calculations of electron inelastic mean free paths. V. Data for 14 organic compounds over the 50–2000 eV range," *Surf. Interface Anal.*, vol. 21, no. 3, pp. 165–176, Mar. 1994, doi: https://doi.org/10.1002/sia.740210302.

[13] J. Müller, T. S. Böscke, U. Schröder, S. Mueller, and D. Bräuhaus, "U. Böttge r, L. Frey, T. Mikolajick, Ferroelectricity in Simple Binary ZrO2 and HfO2," *Nano Lett*, vol. 12, pp. 4318–4323, 2012.

[14] J. Müller *et al.*, "Ferroelectricity in simple binary ZrO2 and HfO2," *Nano Lett.*, vol. 12, no. 8, pp. 4318–4323, Aug. 2012.

[15] W. Hamouda *et al.*, "Oxygen vacancy concentration as a function of cycling and polarization state in TiN/Hf0.5Zr0.5O2/TiN ferroelectric capacitors studied by x-ray photoemission electron microscopy," *Appl. Phys. Lett.*, vol. 120, no. 20, 2022.

[16] X. Henning *et al.*, "Oxygen vacancy effects on polarization switching of ferroelectric Bi2FeCrO2 thin films," *Phys. Rev. Mater.*, vol. 8, no. 5, p. 54416, May 2024, doi: 10.1103/PhysRevMaterials.8.054416.

[17] J. P. B. Silva *et al.*, "Roadmap on ferroelectric hafnia- and zirconia-based materials and devices," *APL Mater.*, vol. 11, no. 8, 2023.

[18] P. E. Bloomfield, I. Lefkowitz, and A. D. Aronoff, "Electric field distriutions in dielectrics, with special emphasis on near-surface regions in ferroelectrics," *Phys. Rev. B*, vol. 4, no. 3, p. 974, 1971.

[19] A. Morozzi, M. Hoffmann, R. Mulargia, S. Slesazeck, and E. Robutti, "Negative capacitance devices: sensitivity analyses of the developed TCAD ferroelectric model for HZO," *J. Instrum.*, vol. 17, no. 01, p. C01048, 2022.

[20] R. Materlik, C. Künneth, and A. Kersch, "The origin of ferroelectricity in Hf1− xZrxO2: A computational investigation and a surface energy model," *J. Appl. Phys.*, vol. 117, no. 13, 2015.

[21] G. Greczynski and L. Hultman, "Towards reliable X-ray photoelectron spectroscopy: sputter-damage effects in transition metal borides, carbides, nitrides, and oxides," *Appl. Surf. Sci.*, vol. 542, p. 148599, 2021.